Anomalous magnetic properties of brain tissue at low temperature: The 50 K anomaly

Ann M. Hirt,[1] Franziska Brem,[1] Marianne Hanzlik,[2] and Damien Faivre[3]

Received 15 June 2006; revised 2 October 2006; accepted 25 October 2006; published 7 December 2006.

[1] A low-coercivity phase, identified as magnetite and/or maghemite, is the main iron oxide in brain tissue. Measurement of susceptibility as a function of temperature (χ–T) in brain tissue samples does not show a Verwey transition but instead shows a perturbation around 50 K. A susceptibility anomaly has been reported at this temperature in several studies of multidomain magnetite crystals, which, however, also display a Verwey transition. We have investigated the magnetic characteristics of this 50 K anomaly further in brain and tumor tissue. The magnetic measurements consist of χ–T curves, measured after cooling in zero field (ZFC) or in a field (FC), as well as hysteresis loops. The 50 K anomaly is expressed as a bump in χ–T curves over a 20 K temperature range, with a peak between 44 and 58 K. The magnetic intensity of the samples is weak; however, the anomaly signal is an order of magnitude larger than known effects related to the magnetic ordering of oxygen at 43 K. A phase transition, or magnetic ordering of another phase, does not seem a likely explanation, because both the ZFC and FC curves follow the perturbation, rather than showing a bifurcation at peak susceptibility. This explanation also precludes magnetic blocking of a superparamagnetic component. Hysteresis loops at temperature of the peak perturbation show a splitting of the descending and ascending limbs at the maximum starting field. The magnetic behavior observed in these experiments is consistent with a change in electron activity.

Citation: Hirt, A. M., F. Brem, M. Hanzlik, and D. Faivre (2006), Anomalous magnetic properties of brain tissue at low temperature: The 50 K anomaly, *J. Geophys. Res.*, *111*, B12S06, doi:10.1029/2006JB004570.

1. Introduction

[2] There is a long history of geophysical interest in the magnetic properties of magnetite, because of its role as a stable recorder of the Earth's magnetic field over geologic time. Magnetite has also been investigated outside the geophysics community, due to its use in traditional magnetic recording media. Recently, there has been an increase in interest in magnetite because it can be used for high-spin polarized transport, which is desirable in tunneling magnetoresistance devices and spintronics [e.g., *Gupta and Sun*, 1999; *Seneor et al.*, 1999]. Low-temperature magnetic properties of magnetite have been examined extensively for more than 65 years. *Verwey* [1939] noted a discontinuous transformation around 125 K, in the form of an abrupt decrease in electrical conductivity by 2 orders of magnitude, and a change in crystal structure from cubic to monoclinic below this temperature. Detailed reviews of the Verwey transition are given by *Walz* [2002] and *García and Subías* [2004]. The Verwey transition occurs close to the temperature at which the magnetocrystalline anisotropy changes sign, forming an isotropic point around 130 K [e.g., *Kobayashi and Fuller*, 1968; *Moskowitz et al.*, 1998].

[3] The increased availability of high-sensitivity magnetometers capable of measuring at low temperatures has led to an increase in the number of studies of the low-temperature magnetic properties of magnetite-bearing materials. The occurrence of a Verwey transition in low-temperature measurements of induced magnetization is often used in the paleomagnetic and rock magnetic communities as a criterion for the presence of magnetite. In the physics and material science communities, interest has recently focused on the magnetic properties of magnetite over a range of temperatures below the Verwey transition, because of its spin polarization [e.g., *Skumryev et al.*, 1999; *Seyoum et al.*, 2003; *Balanda et al.*, 2005; *Walz et al.*, 2005].

[4] Magnetic aftereffect (MAE) has been used in a series of studies to examine relaxation processes below the Verwey transition in stoichiometric and Ti-doped, multidomain (MD) magnetite [cf. *Walz*, 2002; *Walz et al.*, 2005, and references therein].There are no reported measurements made explicitly on single-domain magnetite. MAE reflects the relaxation of initial susceptibility and arises from thermally activated magneto-electronic relaxation processes due to (1) time-dependent magnetocrystalline interaction of spontaneous wall magnetization in single crystals with large numbers of identical anisotropic lattice defects and (2) inherent coupling of local charge and anisotropy transport between neighboring B-sited iron ions of differ-

[1] Institute of Geophysics, ETH-Zürich, Zürich, Switzerland.
[2] Technische Chemie 1, Technische Universität München, Gärching, Germany.
[3] Max Planck Institute for Marine Microbiology, Bremen, Germany.

0148-0227/06/2006JB004570$09.00

ent valencies [*Walz et al.*, 2005]. MAE data suggest that three relaxation processes may occur in different temperature ranges below the Verwey transition in stoichiometric magnetite. These are (1) incoherent electron tunneling between 4 K and 20 K, (2) intraionic excitation at around 30 K, and (3) variable range electron hopping between 50 K and the Verwey transition at 125 K. The temperature range between 35 K and 50 K is characterized by a relaxation hiatus. *Walz et al.* [2005] showed that adding small amounts of Ti to magnetite (forming $Fe_{3-x}Ti_xO_4$; x = 0.0001–0.0080) inhibits low-temperature tunneling. The initial susceptibility of the stoichiometric magnetite was also monitored in these studies; a steep drop was found at the Verwey transition, followed by a plateau from 125 K to 50 K and then a further smaller drop in intensity; finally, there was a slight increase below 30 K. Adding Ti reduced the drop in susceptibility seen at the Verwey transition and also shifted the transition to lower temperature. The further drop at 50 K was also reduced and the susceptibility remained low until 4 K.

[5] *Moskowitz et al.* [1998] investigated the AC susceptibility in low temperature for a series of synthetic MD titanomagnetites. For a pure magnetite sample they found a pronounced drop in susceptibility at the Verwey transition, followed by a slight increase and a second smaller drop between 50 K and 60 K. In a study of pure magnetite crystals with grain sizes between 0.05 μm and 108 μm, *Muxworthy* [1999] also observed a drop in the AC susceptibility below 50 K. The drop was more pronounced in the MD samples but was also present, although very weak, in his single-domain (SD) sample. Both studies referred to the MAE results of *Walz and Kronmüller* [1991] with respect to the results around 50 K, but they did not try to interpret further this anomalous behavior.

[6] *Balanda et al.* [2005] monitored AC susceptibility between 4 K and 200 K in stoichiometric and Zn-doped single crystals of magnetite. The $Fe_{3-x}Zn_xO_4$ crystals had Zn substitution values x in the range x = 0.0072–0.0490. In-phase susceptibility (χ') of the stoichiometric crystal resembled the initial susceptibility data from *Walz et al.* [2005]. Doping the crystals with Zn suppressed the drop in χ' observed at 50 K. The out-of-phase susceptibility (χ'') showed a broad peak between approximately 40 K and 60 K, which has a frequency dependence. The lower the frequency, the lower the temperature at which the peak was found. The decrease in χ' and increase in χ'' was suppressed in higher applied AC fields.

[7] Recent investigations of the magnetic properties of human brain tissue, which had been resected either during amygdalohippocampectomies from patients suffering from mesial temporal lobe epilepsy (MTLE) [*Wieser and Yasargil*, 1981] or for tumor removal, have shown the presence of magnetite/maghemite and ferritin, an iron storage protein that consists of a ferrihydrite core surrounded by a protein shell, and heme-iron (blood) [*Brem et al.*, 2005a, 2005b]. The magnetic signal in the brain tissue is very weak, so it is only possible to measure DC susceptibility as a function of temperature. A Verwey transition has not been identified in any of the samples, but an anomalous bump in the susceptibility curve around 50 K is found in all samples. In the present study further magnetic measurements were made in the temperature range of the susceptibility anomaly in order to gain a better understanding about the origin of this anomalous behavior.

2. Samples and Methods

[8] The samples used in this study include seven hippocampal tissues; three samples showed no pathogenesis and were obtained from autopsies; four samples were resected from MTLE patients (Table 1). Ten tumor tissues were also examined, of which seven were meningiomas (Table 1). All samples were resected at the Department of Neurosurgery, University Hospital Zurich, and all procedures were conducted in accordance with the Declaration of Helsinki and approved by the ethics committee of the Canton Zurich. Nonpathogenic brain tissue from a mouse was obtained from the Institute of Toxicology and Pharmacology, University of Zurich and also examined.

[9] Tissue samples were frozen in liquid nitrogen immediately after resection and stored at 193 K to prevent chemical alteration of the iron mineralogy. Subsequently the tissue was freeze-dried for the measurements. Following the procedures outlined by *Dobson and Grassi* [1996] and *Brem et al.* [2005b], special precaution was taken to prevent any contamination.

[10] Measurements were made with a Quantum Design Magnetic Property Measurement System (MPMS) SQUID magnetometer at the Institute for Geosciences, University of Bremen, Institute of Rock Magnetism, University of Minnesota, and the Chemistry Department, ETH Zurich. The three magnetometers are equipped with an internal field compensation coil so that the residual field is less than 100 μT. In one set of experiments induced magnetization was measured as a function of temperature between 5 K and 300 K in a 50 mT field after the sample was cooled in zero field (ZFC) or cooled in an applied field of 50 mT (FC). Two samples, HA1 and SG2, were first cooled to 5 K in a field of 50 mT, and then rewarmed in a 50 mT field as above, but subsequently the induced magnetization was measured between 300 and 5 K during recooling in a 50 mT field.

[11] The induced magnetization was also measured as a function of field (hysteresis loops) at a series of temperatures between 5 K and 300 K (Table 1). The measurements were normally started at the maximum positive field of 5 T. For one loop at 50 K, the hysteresis measurement was started at the maximum negative field of −5 T.

[12] To aid in identification of the iron phases that were magnetically ordered at room temperature, a magnetic separation was made using the method of *Grünberg et al.* [2004] for the isolation of magnetosomes. Resolubilization of the sample and magnetic separation were carried out on two samples (HA1 and SG) as follows. The sample was introduced in a 1.5 mL tube, and 500 μL of a 50 mM HEPES buffer (pH = 7.4) and 10 μL of proteinase K (Macherey-Nagel) were added. The proteinase K was left overnight 15 hours at 50°C and agitated at 1200 rpm to dissolve the sample. It was then centrifuged for 5 min at 14,000 rpm, and 450 μL were removed. The pellet was resuspended using the same buffer and centrifuged again under the same conditions. Once again, 450 μL of the supernatent were removed, the pellet was resuspended in the remaining 50 μL and introduced in a MACS magnetic

Table 1. Description of Samples[a]

Sample	Weight After Freeze-Drying, mg	Days Between Freeze-Drying and Measurement	Hysteresis Loops at Specified Temperature	Peak Temperature of Anomalies for ZFC, K
		Hippocampus		
AK	124	6	5, 50, 300	48
ES1	81	104	5, 45, 54, 57, 77, 300	45, 57
IR	72	6	5, 25, 45, 55, 77, 300	44, 54
SG1	83	23	-	50
274 Hc autopsy	45	9	5, 25, 54, 77, 300	54
275 Hc autopsy	19	11	5, 25, 45, 54, 300	45, 55
275 Hc[b]	37	20[c]		45
275 Pc autopsy	104	9	-	55
		Tumors		
GH Astrozytom	94	8	5, 25, 77, 300	48
GH2 Meningioma	66	106	5, 48, 300	49
GS Oligoastrozytom	37	25	-	45, 54
GS[b]	37	8[c]		53
HA1 Meningioma	32	108	5, 30, 40, 59, 60, 300	49
HM2 Meningioma	106	68	5, 300	51
HT Haemangioma	40	23	5, 25, 54, 300	54
KF Meningioma	158	109	5, 49, 300	49
NB Meningioma	112	70	5, 300	50
NU	112	7	5, 25, 300	48
SG2 Meningioma	28	107	5, 49, 300	49
		Mouse Brain		
M1	101	8	5, 45, 58, 300	

[a]Astrozytom and Oligoastrozytom are intracranial tumors; meningioma is a tumor on the outermost layer of the skin of the brain; and haemangioma is a dense collection of blood vessels associated with a lesion.
[b]Samples that were stored at room temperature under humid conditions.
[c]Number of days in storage.

separation column (Miltenyi Biotec). The column was placed between two Sm-Co magnets, which generated a magnetic field that magnetized the column wire matrix, thereby trapping the magnetic particles in the matrix. The pellet was first washed in the magnetized column with 3 × 1 mL of extraction buffer, which consisted of a solution of 10 mM HEPES, 1 mM EDTA, and 0.1 mM PMSF, with pH = 7.4. After the magnets were removed from the column, magnetic particles were eluted with 3 × 500 μL of the same extraction buffer. The 1.5 mL were then centrifuged at 14,000 rpm for 5 min, and 1.4 mL of the supernatant was removed. The magnetic particles were then resuspended in the final 100 μL and a drop was deposed on a 300 mesh C-Cu grid for transmission electron microscope (TEM) analysis. TEM micrographs and selected area electron diffraction patterns (SAED) were taken on a JEOL JEM 2010 operating at 120 kV.

3. Results

3.1. Magnetic Mineralogy

[13] A detailed analysis of the magnetic mineralogy of the pathogenic hippocampal and mengioma tissues has been reported by *Brem et al.* [2006b]. In this study, acquisition of an isothermal remanent magnetization (IRM) was used to identify the low-coercivity phase, magnetite and/or maghemite, that is magnetically ordered at 77 K and at room temperature (293 K). The IRM experiments indicate that all tissues contain a low-coercivity ferrimagnetic phase that is magnetically saturated by 250 mT (Figure 1). The intensity of the saturation remanent magnetization (M_{rs}) increases on cooling to 77 K from 293 K. The shape of the acquisition curve is the same at both temperatures, which suggests that a single mineral phase is present at 77 K and above. The increase in M_{rs} at low temperature is due to blocking of finer particles that are superparamagnetic at room temperature. A second magnetic phase, ferritin, only starts to undergo magnetic ordering below 22 K. The nonpathogenic hippocampal tissue had magnetic properties similar to the pathogenic hippocampal tissue.

3.2. Induced Magnetization Versus Temperature

[14] As seen in earlier studies, the induced magnetization after ZFC and FC shows a rapid loss in magnetization on rewarming between 2 K and 8 K, which is attributed to a paramagnetic signal from blood in the tissue (Figure 2). The

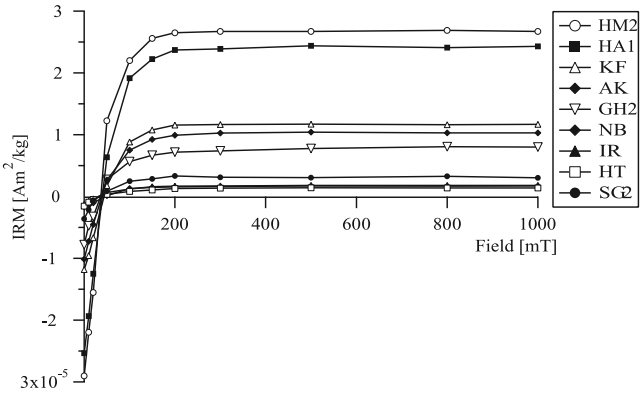

Figure 1. Acquisition of isothermal remanent magnetization (IRM) for a selection of tissue samples.

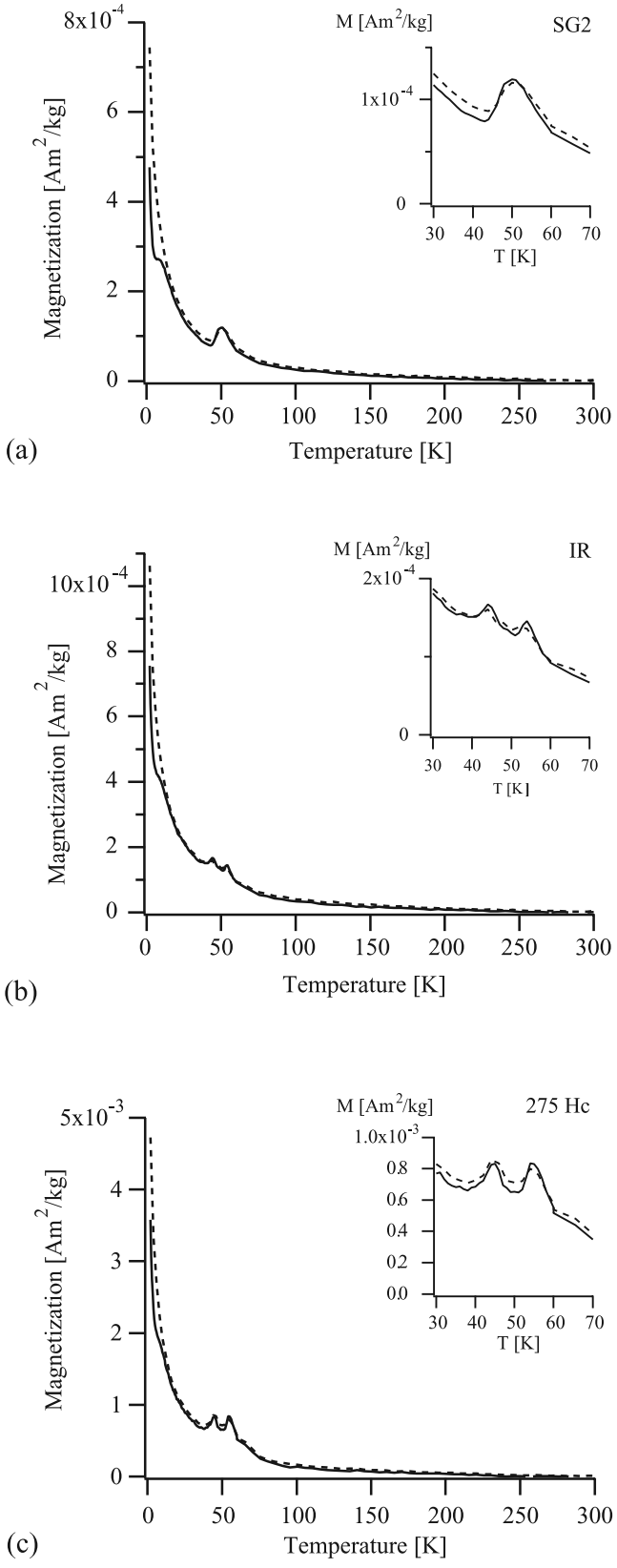

Figure 2. Induced magnetization as a function of temperature for ZFC (solid line) and FC (dashed line) for a representative hippocampus samples showing (a) a single susceptibility peak and a double susceptibility peak for (b) pathogenic and (c) nonpathogenic tissue.

plateau in the ZFC magnetization curve between 9 K and 12 K is the mean magnetic ordering temperature of ferritin [*Brem et al.*, 2005b, 2006b]. The maximum unblocking temperature of the ferritin component derived from the ZFC and FC curves is around 22 K.

[15] With further warming, a perturbation is seen between 40 K and 60 K. It is found in both the ZFC and FC magnetization (Figure 2, insets). For some tissue samples this anomalous behavior is expressed as a single perturbation (Figure 2a), and in other samples it is expressed as a double perturbation (Figure 2b). Whether a single or double perturbation was present appeared to be unrelated to the type of tissue, to the storage time between resection and freeze-drying, or to the time between freeze-drying and measurement (Table 1). Nonpathogenic tissue also displayed a perturbation in the induced magnetization (Figure 2c). If the samples were stored at room temperature in a humid environment, changes were observed in the peak of the perturbation. In the case of a single perturbation, the intensity of the peak decreased but remained at the same temperature. In the case of a double perturbation, the higher temperature anomaly disappeared and only the lower temperature anomaly remained (Figure 3).

[16] In two samples from tumor tissues (HA1, SG2), the temperature of the peak in the FC curve was shifted with respect to the peak in the ZFC curve (Figure 4). For both these samples, the FC experiment was measured during warming from 5 K to 300 K as well as during cooling from 300 K to 5 K. In the warming experiment, the anomaly shifted to a temperature slightly higher than observed in the ZFC curve; in the cooling experiment, the anomaly shifted to a slightly lower temperature than in the ZFC curve.

[17] Similarly, the brain tissue from a mouse displays a well-defined anomaly at 58 K. The magnetic ordering of a ferritin component is not obvious for this sample, which may indicate that its mean blocking temperature is below 5 K.

3.3. Magnetization Versus Field

[18] Magnetization was measured as a function of field at a series of temperatures (Table 1), particularly between 30 K and 60 K. At 5 K the hysteresis loop is dominated by the ferritin component [*Brem et al.*, 2005b, 2006b]. There is a slight constriction in the curve, due to the low-coercivity component (Figure 5). By 30 K the ferritin is unblocked and only the low-coercivity phase, magnetite/maghemite, is magnetically ordered (Figure 6a, right). The low-coercivity phase reaches magnetic saturation by 200–250 mT. The high-field part of the curve, arising from the unblocked ferritin component, has a susceptibility of 3.91×10^{-9} m^3/kg. At 40 K the hysteresis loop displays a bifurcation in the descending and ascending limbs of the curve in positive fields in addition to a small open loop in low field (Figure 6b). The ascending and descending limbs in negative fields have the same slope. At 50 K, close to the maximum perturbation, the bifurcation between the two curves increases (Figure 6c). Whether the hysteresis curve starts on the upper limb or lower limb is dependent on previous treatment. For example, the measurement shown in Figure 6c started on the upper limb and returned on the lower limb. The hysteresis measurement was run again at the same temperature and in this second run it started on the lower limb and

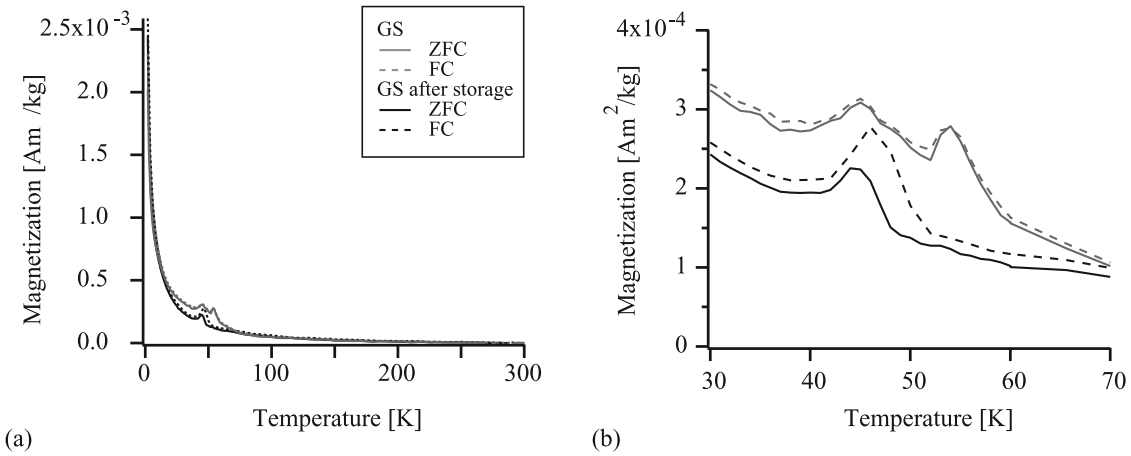

Figure 3. Induced magnetization as a function of temperature for ZFC (solid line) and FC (dashed line) for sample GS, showing (a) a double susceptibility peak before storage and (b) a single peak after storage.

returned on the upper limb. A further hysteresis measurement was started at the maximum negative field strength. In this case the bifurcation was found in the negative field part of the curve, which indicates the bifurcation occurs on the initial descending and ascending parts of the curve (Figure 6c, right). At 60 K the bifurcation is again reduced and the slope of the high-field part of the curve returns to values similar to those seen below 40 K (Figure 6d). Although the sample HA was not measured at 77 K, hysteresis curves of other samples do not show any bifurcation, and reflect the superparamagnetic contribution of the ferritin component with a component due to the low-coercivity phase.

[19] A similar bifurcation in the initial hysteresis loops was also seen in the nonpathogenic hippocampal tissue and the mouse brain tissue at the peak of the susceptibility anomaly (Figures 7a and 7b).

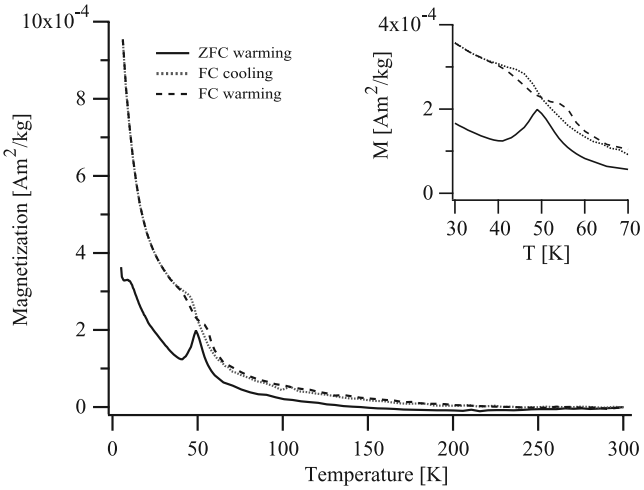

Figure 4. Induced magnetization as a function of temperature for ZFC (solid line), FC warming (dashed line), and FC cooling (dotted line) for sample HA1.

3.4. Microscopy

[20] A copper grid was analyzed with particles extracted from tumor tissue. A cluster that consists of small particles between 5 and 30 nm was found, together with residue from dissolution of the organic material (Figure 8a). Distinct cubic grains can be discerned in the upper part of the bright-field image. A SAED pattern made on the particle cluster was characteristic of a fine-grained cubic crystalline material, which could be magnetite or maghemite (Figure 8b). The d spacings are given in Table 2, and the values are compatible with magnetite. Further work is needed to confirm this first observation.

4. Discussion

[21] A study on human hippocampus and tumor tissue, as well as mouse brain tissue, displays anomalous behavior in the DC magnetization around 50 K. Earlier studies have shown that there are several iron phases in brain and tumor tissue [*Kirschvink et al.*, 1992a, 1992b; *Dunn et al.*, 1995;

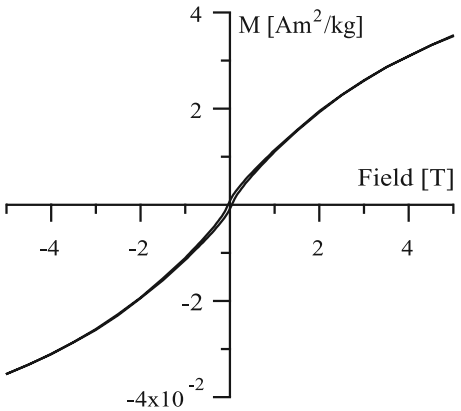

Figure 5. Induced magnetization as a function of field for sample HA1 at 5 K.

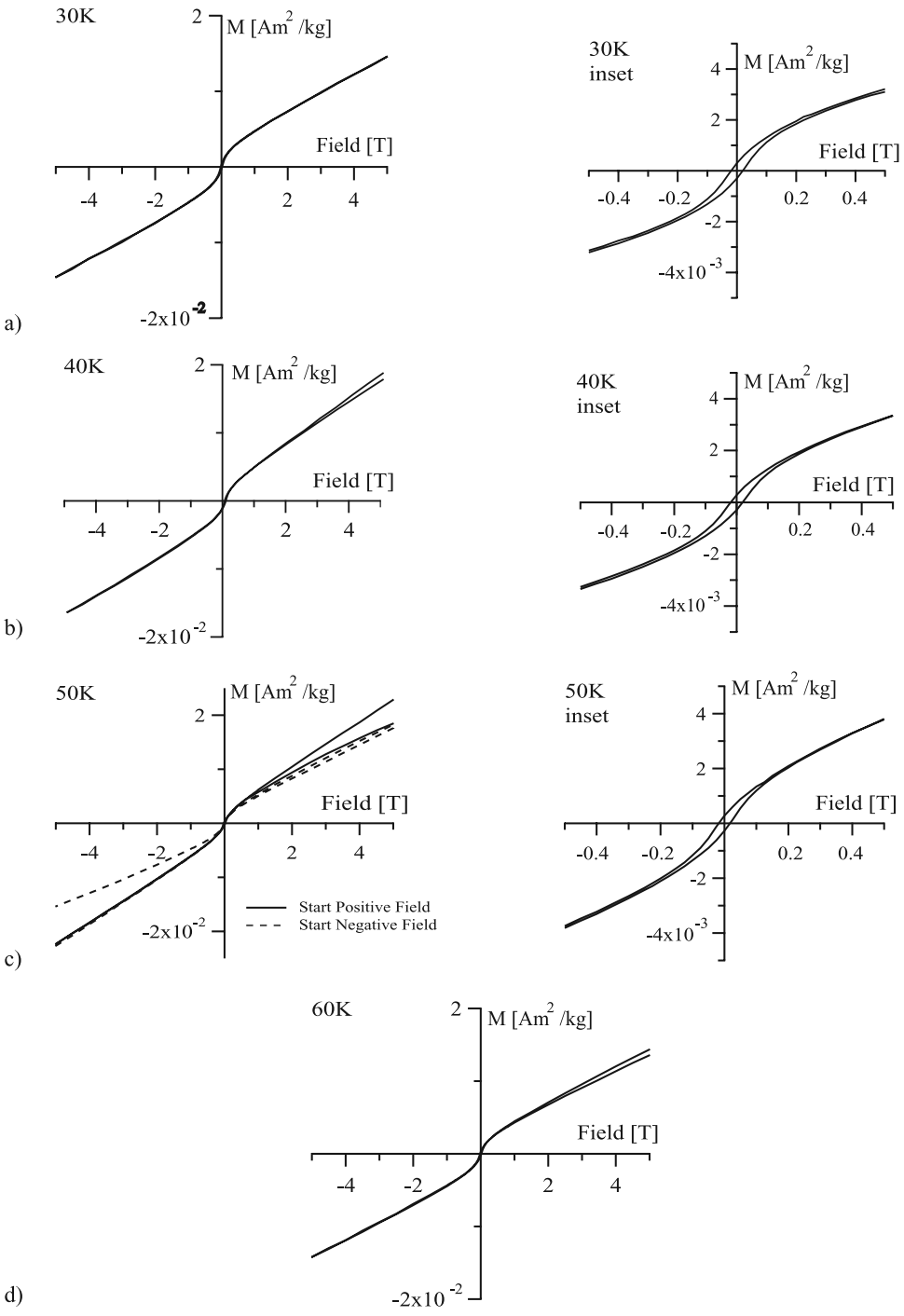

Figure 6. Induced magnetization as a function of field for sample HA1 at (a) 30 K, (b) 40 K, (c) 50 K, and (d) 60 K.

Dobson and Grassi, 1996; *Dubiel et al.*, 1999; *Schultheiss-Grassi and Dobson*, 1999; *Quintana et al.*, 2000, 2004, 2006; *Hautot et al.*, 2003; *Brem et al.*, 2005a, 2005b, 2006b]. They include heme-iron in blood, ferritin, a magnetite/maghemite hemosiderine, which is a degraded, insoluble form of ferritin, and wustite. Measurements on blood samples show that plots of inverse susceptibility as a function of temperature deviate slightly from linear dependence, but the deviation is not significant [*Mosiniewicz-Szablewska et al.*, 2003; *Slawska-Waniewska et al.*, 2004; *Brem et al.*, 2005a]. For this reason, blood is considered to have a quasi-paramagnetic magnetization at temperatures above 2 K. Ferritin in brain samples shows magnetic ordering between 8 K and 12 K and final unblocking on warming is between 22 K and 38 K [*Dubiel et al.*, 1999; *Brem et al.*, 2005b]. Above this temperature, ferritin shows Langevin behavior [*Brem et al.*, 2006a], and so cannot contribute to the observed anomaly around 50 K.

[22] A low-coercivity ferrimagnetic phase has been identified in the above studies. Although a Verwey transition has

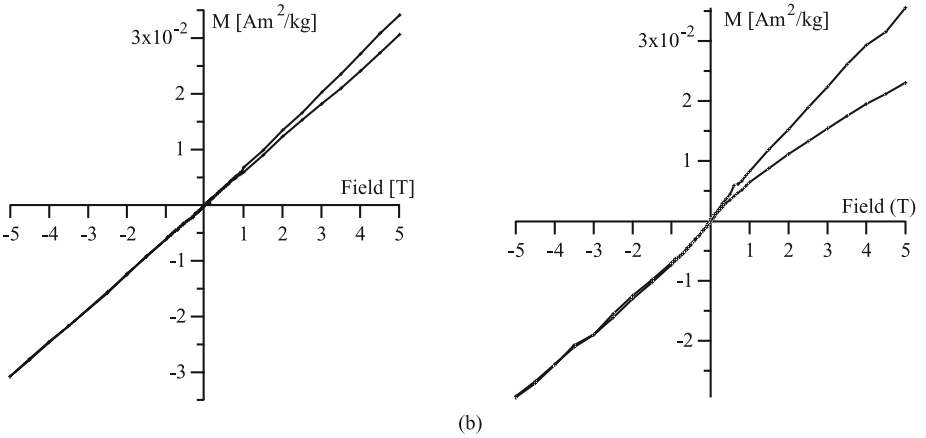

Figure 7. Induced magnetization as a function of field for (a) nonpathogenic hippocampal tissue at 54 K and (b) mouse brain tissue at 58 K.

only been identified in some studies, X-ray diffraction has shown this phase to be magnetite and or maghemite [*Kirschvink et al.*, 1992a, 1992b; *Dunn et al.*, 1995; *Schultheiss-Grassi et al.*, 1999; *Quintana et al.*, 2000, 2004]. *Quintana et al.* [2004; 2006] have identified magnetite/maghemite and wustite in ferritin cores. Of these phases, the only iron phase that has shown an anomalous behavior in magnetic properties around 50 K is magnetite, either from measurement of MAE [*Walz and Kronmüller*, 1991; *Walz et al.*, 1997] or AC susceptibility [*Moskowitz et al.*, 1998; *Muxworthy*, 1999; *Skumryev et al.*, 1999; *Balanda et al.*, 2005]. MAE experiments identify a gap in relaxation processes between 30 K and 50 K, which is followed by the onset of thermally activated electron hopping above 50–60 K [e.g., *Walz et al.*, 2005]. This is expressed as a sudden small increase in the AC susceptibility around 50–60 K upon warming. The AC susceptibility is frequency-dependent, which is compatible with a thermally activated process [*Skumryev et al.*, 1999; *Balanda et al.*, 2005]. The anomaly is depressed for nonstoichiometry or doping with other cations. All of the aforementioned studies examined MD magnetite; studies on SD magnetite show that this effect is less pronounced [*Muxworthy*, 1999].

[23] Anomalous behavior in the magnetic properties of magnetite at 50 K is also seen in epitaxial films with thicknesses <10 nm [*van der Heijden et al.*, 1998]. The films did not show anisotropic behavior in their ferromagnetic resonance, as opposed to films with thickness >10 nm. *van der Heijden et al.* [1998] explained this behavior as resulting from a change in the compensation of either magnetizations or angular momenta on the sublattices. They also noted that the Verwey transition is suppressed for film thicknesses under 5 nm.

[24] Studies on the electrical properties of MD single crystals of magnetite also identify an anomaly in the magnetoelectrical polarization around 45 K [*Inase and Miyamoto*, 1987], which disappeared above approximately 50 K. The authors of these studies concluded that the observed behavior was due to a switching of the *a* and *b* axes around this temperature, possibly induced by the rearrangement of Fe^{2+} and Fe^{3+} ions, due to the application of a magnetic field.

[25] Although the present investigation does not provide a definitive explanation for the anomalous behavior in the magnetization around 50 K, it is possible to suggest mechanisms that would be responsible for the observed results. A simple explanation is that this behavior is instrumental in origin. We do not believe that this is the case, for several reasons. First, the same behavior has been observed using three different Quantum Design MPMS magnetometers, and, secondly, the anomaly occurs over a range of magnetization intensities, so that it does not appear to be related to a change in the measurement range in response to a change in magnetization intensity. In addition, the anomaly has not been observed in other biomagnetic material measured on these instruments, such as magnetotactic bacteria that were measured on the MPMS magnetometer in Bremen [cf. *Pan et al.*, 2005].

[26] Another explanation for the anomalous behavior of the induced magnetization in the tissue would be the magnetic ordering of an unidentified phase. A non-iron phase that shows a magnetic transition at 43 K is oxygen, which changes from paramagnetic to antiferromagnetic around this temperature [*Schubert*, 1978]. If a small air leak occurs in the system, air can accumulate in the sample chamber. Below 100 K the walls of the chamber, straw or sample itself might act as a cryopump and cause the incoming oxygen to condense on the cold surface. However, none of the three magnetometers was found to have an air leak in the system. Care was taken in evacuating the sample chamber before each measurement, and in most cases the chamber was purged several times, so that any oxygen outgassing from the sample would be removed. To further test the possibility of oxygen contamination, a sample of palladium was prepared in a sealed sample tube after introducing air. The induced magnetization was measured as a function of temperature by first cooling the sample from 300 to 2 K and then rewarming back to 300 K (Figure 9). No anomaly appears in the magnetization upon cooling, and upon warming, there is a broad anomaly with a peak at 63 K. It should be noted that this signal is an order of magnitude smaller than the anomaly observed in the hippocampus and tumor tissues. Important is that the anomaly in the tissue samples was seen in both warming and cooling curves

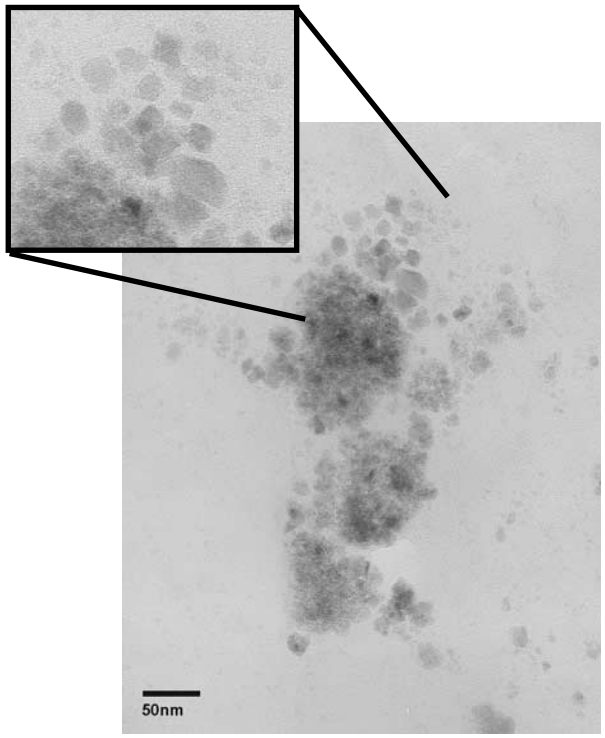

(a)

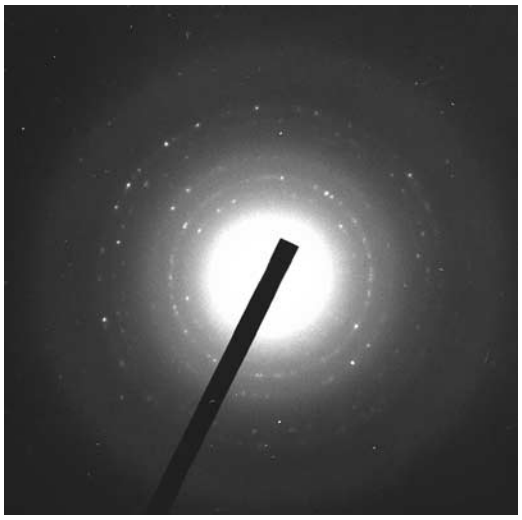

(b)

Figure 8. (a) TEM micrograph of a cluster of nanosized iron oxide particles that were extracted from HA1. (b) Corresponding SAED pattern.

Table 2. Comparison of Experimentally Observed d Spacings (in nm) in SAED Determinations on the Tissue Samples and Theoretical Values for Magnetite JCPDS[a]

Brain Tissue Extract	Theoretical
0.296	0.297
0.252	0.253
0.209	0.210
0.162	0.162
0.148	0.148

[a]The d spacings are in nm. JCPDS, Joint Committee on Powder Diffraction Standards.

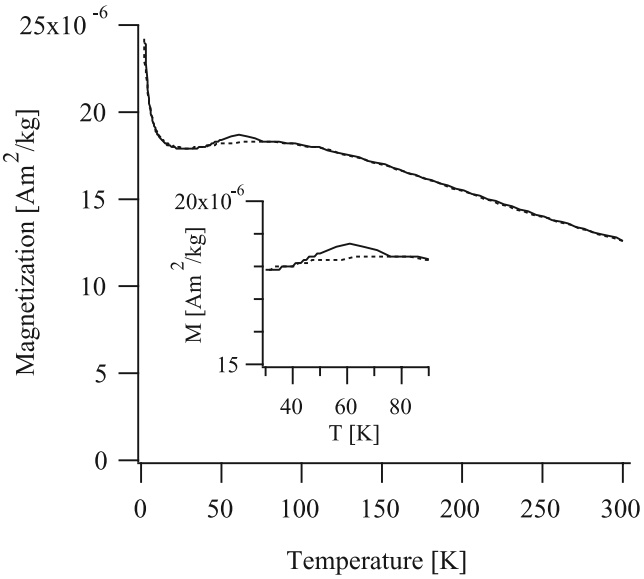

Figure 9. Induced magnetization as a function of temperature for ZFC warming (solid line) and cooling (dashed line) for a sample of palladium in oxygen.

(Figure 3). Moreover, if the anomaly were due to a transition from paramagnetic to antiferromagnetic state, then the FC curve should not decrease after cooling through the temperature of peak magnetization in the ZFC curve, but should continue to increase.

[27] Alternatively another unidentified (iron) phase could be present in the tissues. In this case, the ZFC curve would show a peak in the induced magnetization curve, but, as stated above, the FC curve should show a continuous increase in magnetization upon cooling below the perturbation, as seen in the magnetic ordering of the ferritin around 11 K.

[28] This behavior does not appear to be associated with ferritin, since ferritin is no longer ordered above approximately 22 K. No similar anomalous behavior in susceptibility has been seen in investigations on a variety of ferritin samples [e.g., *Allen et al.*, 2000; *Seehra et al.*, 2000; *Seehra and Punnoose*, 2001; *Brem et al.*, 2006a]. Wustite has a Néel temperature around 198 K and nanoparticles should produce a broader peak, unless a very limited grain size was present. Magnetic ordering of an unidentified iron phase would not support the behavior of magnetic hysteresis in the temperature range in which the anomaly is seen in the induced magnetization.

[29] The observation that the double peak was reduced to a single peak after storage at room temperature under humid conditions, which would promote oxidation (Figure 2), suggests that the behavior is related to composition of the phase. A long-term storage test would be necessary to determine if all anomalous behavior around 50 K disappears when left in ambient conditions for a lengthy period, as the sample underwent further oxidation. It should be noted that our samples were always stored at 193 K. Special care was taken during freeze-drying to avoid exposing any sample to temperatures above 273 K. The samples were also not ground after freeze-drying. Under these conditions measurement of the anomaly is repeatable.

[30] As noted above, anomalous behavior has been identified in AC susceptibility, MAE, and magnetoelectric polarization of MD magnetite, and in the ferromagnetic resonance of thin films <10 nm in thickness between 40 K and 60 K. This behavior has been associated with the onset of electron hopping upon warming and ionic ordering within domain walls, which start to conform to wall movement. The particle size in the tumor and hippocampal tissue is most likely to be finer grained. Measurements of first-order reversal curves (FORC) suggest that the tumor tissue is characterized by single-domain and superparamagnetic grain size, and that the hippocampus is dominated by superparamagnetic grain sizes [*Brem et al.*, 2006b]. For this reason, it is unlikely that domain walls are involved. However, rearrangement of cations on sublattices or in electron configuration cannot be ruled out. *Inase and Miyamoto*'s [1987] suggestion that there is a switching of the *a-b* axes around 45 K, could possibly explain the bifurcation seen in the hysteresis loops. In the initial field, the easy axis of magnetization would lie along one of the axes. As the field is decreased and then increased to the starting value, there could be a switch, leading to the observed change in susceptibility. When starting again, the magnetization would start at the value of the last state and then switch back to the previous state after going through a cycle.

[31] Further experimentation is necessary to verify this model. It is interesting to note that the 50 K anomaly has not been seen in most experiments on synthetic magnetite with grain sizes under 30 nm. If it proves possible to extract enough of the iron mineralogy from tissue samples, it would be possible to use AC susceptibility measurements versus temperature or other spectroscopic methods, e.g., electron spin resonance spectroscopy (ESR) or neutron diffraction. Spectroscopic studies would provide valuable information on processes occurring between 40 K and 60 K on the atomic level. It must be noted, however, that limited tissue material are available for these studies, and due to the low concentration, a large pool of samples would be necessary for other methods, that require higher concentrations.

5. Conclusions

[32] Tissues from human hippocampus and tumors and from mouse brains display an anomalous peak in susceptibility from approximately 40 K to 60 K. In addition, hysteresis loops in this temperature range show a bifurcation in the ascending and descending limbs on the initial field side of the loop. This behavior is not related to magnetic ordering or blocking of a particular phase since the perturbation is seen in the induced magnetization as a function of temperature after both ZFC and FC treatments. It appears rather to be related to a fundamental change in electron activity in magnetite, as observed in MAE measurements and magnetoelectrical properties.

[33] **Acknowledgments.** The authors thank and P. Solheid and M. Jackson and the Institute of Rock Magnetism at the University of Minnesota, T. Fredericks and the Institute for Geosciences at the University of Bremen, and A. Weber at the Chemistry Department at the ETH-Zürich for the use of the MPMS. A. Weber is also thanked for providing measurements of oxygen contamination of a palladium sample on the MPMS. W. Lowrie is acknowledged for his helpful comments. We also acknowledge helpful comments by C. Carvallo and an anonymous reviewer. D. Faivre acknowledges support from a Marie Curie Fellowship from the European Union (project BacMag). The project was supported by ETH Project 0-20118-03. ETH contribution 1477.

References

Allen, P. D., T. G. St Pierre, W. Chua-anusorn, V. Strom, and K. V. Rao (2000), Low-frequency low-field magnetic susceptibility of ferritin and hemosiderin, *Biochim. Biophys. Acta*, *1500*, 186–196.

Balanda, M., A. Wiechec, D. Kim, Z. Kakol, A. Kozlowski, P. Niedziela, J. Sabol, Z. Tarnawski, and J. M. Honig (2005), Magnetic AC susceptibility of stoichiometric and low zinc doped magnetite single crystals, *Eur. Phys. J. B*, *43*, 201–210.

Brem, F., A. M. Hirt, C. Simon, H. G. Wieser, and J. Dobson (2005a), Characterization of iron compounds in human brain tumour tissue from epileptic patients using low temperature magnetic methods, *J. Phys. Conf. Ser.*, *17*, 61–64.

Brem, F., A. M. Hirt, C. Simon, H. G. Wieser, and J. Dobson (2005b), Characterization of iron compounds in tumour tissue from temporal lobe epilepsy patients using low temperature magnetic methods, *Biometals*, *18*, 191–197.

Brem, F., G. Stamm, and A. M. Hirt (2006a), Modeling the magnetic behavior of horse spleen ferritin with a two-phase core structure, *J. Appl. Phys.*, *99*, 123906.

Brem, F., A. M. Hirt, M. Winkelhofer, K. Frei, Y. Yonekawa, H. G. Wieser, and J. Dobson (2006b), Magnetic iron compounds in the human brain: A comparison of tumour and hippocampal tissue, *Interface*, doi:10.1098/rsif.2006.0133, in press.

Dobson, J., and P. Grassi (1996), Magnetic properties of human hippocampal tissue: Evaluation of artefact and contamination sources, *Brain Res. Bull.*, *39*, 255–259.

Dubiel, S. M., B. Zablotna-Rypien, J. B. Mackey, and J. M. Williams (1999), Magnetic properties of human liver and brain ferritin, *Eur. Biophys. J. Biophys. Lett.*, *28*, 263–267.

Dunn, J. R., M. Fuller, J. Zoeger, J. Dobson, F. Heller, J. Hammann, E. Caine, and B. M. Moskowitz (1995), Magnetic material in the human hippocampus, *Brain Res. Bull.*, *36*, 149–153.

García, J., and G. Subías (2004), The Verwey transition—A new perspective, *J. Phys. Condens. Matter*, *16*, R145–R178.

Grünberg, K., E. C. Müller, A. Otto, R. Reszka, D. Linder, M. Kube, R. Reinhardt, and D. Schüler (2004), Biochemical and protemic analysis of the magnetosome membrane in Magnetospirillium gryphiswaldense, *Appl. Environ. Microbiol.*, *70*, 1040–1050.

Gupta, A., and J. Z. Sun (1999), Spin-polarized transport and magnetoresistance in magnetic oxides, *J. Magn. Magn. Mater.*, *200*, 24–43.

Hautot, D., Q. A. Pankhurst, N. Khan, and J. Dobson (2003), Preliminary evaluation of nanoscale biogenic magnetite in Alzheimer's disease brain tissue, *Proc. R. Soc. London, Ser. B*, *270*, S62–S64.

Inase, T., and Y. Miyamoto (1987), Anomalous behavior in temperature dependence of pyroelectric polarization and magnetoelectric polarization of magnetite below 60 K, *J. Phys. Soc. Jpn.*, *56*, 3683–3688.

Kirschvink, J. L., A. Kobayashi-Kirschvink, and B. J. Woodford (1992a), Magnetite biomineralization in the human brain, *Proc. Natl. Acad. Sci. U.S.A.*, *89*, 7683–7687.

Kirschvink, J. L., A. Kobayashi-Kirschvink, J. C. Diazricci, and S. J. Kirschvink (1992b), Magnetite in human tissues—A mechanism for the biological effects of weak Elf magnetic-fields, *Bioelectromagnetics*, *101–113*, suppl. 1.

Kobayashi, K., and M. Fuller (1968), Stable remanence and memory of multi-domain materials with special reference to magnetite, *Philos. Mag.*, *18*, 601–624.

Mosiniewicz-Szablewska, E., A. Slawska-Waniewska, K. Swiatek, N. Nedelko, J. Galazka-Friedman, and A. Friedman (2003), Electron paramagnetic resonance studies of human liver tissue, *Appl. Mag. Res.*, *24*, 429–435.

Moskowitz, B. M., M. J. Jackson, and C. Kissel (1998), Low-temperature magnetic behavior of titanomagnetites, *Earth Planet. Sci. Lett.*, *157*, 141–149.

Muxworthy, A. R. (1999), Low-temperature susceptibility and hysteresis of magnetite, *Earth Planet. Sci. Lett.*, *169*, 51–58.

Pan, Y., N. Petersen, M. Winkelhofer, A. F. Davila, Q. Liu, T. Frederichs, M. Hanzlik, and R. Zhu (2005), Rock magnetic properties of uncultured magnetotactic bacteria, *Earth Planet. Sci. Lett.*, *237*, 311–325.

Quintana, C., M. Lancin, C. Marchic, M. Pérez, J. Martin-Benito, J. Avila, and J. L. Carrascosa (2000), Initial studies with high resolution TEM and electron energy loss spectroscopy studies of ferritin cores extracted from brains of patients with progressive supranuclear palsy and Alzheimer disease, *Cell. Molec. Bio*, *46*, 807–820.

Quintana, C., J. M. Cowley, and C. Marhic (2004), Electron nanodiffraction and high-resolution electron microscopy studies of the structural and

composition of physiological and pathological ferritin, *J. Struct. Biol.*, *147*, 166–178.

Quintana, C., S. Bellefqih, J. Y. Laval, J. L. Guerquin-Kern, T. D. Wu, J. Avila, I. Ferrer, R. Arranz, and C. Patino (2006), Study of the localization of iron, ferritin, and hemosiderin in Alzheimer's disease hippocampus by analytical microscopy at the subcellular level, *J. Struct. Biol.*, *153*, 42–54.

Schubert, S. (1978), Magnetic susceptibility of oxygen adsorbed on graphite, *Phys. Rev. Lett.*, *40*, 723–725.

Schultheiss-Grassi, P. P., and J. Dobson (1999), Magnetic analysis of human brain tissue, *BioMetals*, *12*, 67–72.

Schultheiss-Grassi, P. P., R. Wessiken, and J. Dobson (1999), TEM investigations of biogenic magnetite extracted from the human hippocampus, *Biochim. Biophys. Acta*, *1426*, 212–216.

Seehra, M. S., and A. Punnoose (2001), Deviations from the Curie-law variation of magnetic susceptibility in antiferromagnetic nanoparticles, *Phys. Rev. B*, *64*, 132,410–132,411, 132,414.

Seehra, M. S., V. S. Babu, A. Manivannan, and J. W. Lynn (2000), Neutron scattering and magnetic studies of ferrihydrite nanoparticles, *Phys. Rev. B*, *61*, 3513–3518.

Seneor, P., A. Fert, J.-L. Maurice, F. Montaigne, F. Petroff, and A. Vaurès (1999), Large magnetoresistance in tunnel junctions with an iron oxide electrode, *Appl. Phys. Lett.*, *74*, 4017–4019.

Seyoum, H. M., L. H. Bennett, and E. Della Torre (2003), Temporal and temperature variations of dc magnetic aftereffect measurements of Fe_3O_4 powders, *J. Appl. Phys.*, *93*, 2820–2822.

Skumryev, V., H. J. Blythe, J. Cullen, and J. M. D. Coey (1999), AC susceptibility of a magnetite crystal, *J. Magn. Magn. Mater.*, *196–197*, 515–517.

Slawska-Waniewska, A., E. Mosiniewicz-Szablewska, N. Nedelko, J. Galazka-Friedman, and A. Friedman (2004), Magnetic studies of iron-entities in human tissue, *J. Magn. Magn. Mater.*, *272–276*, 2417–2419.

van der Heijden, P. A. A., M. G. van Opstal, C. H. W. Swueste, P. H. J. Bloemen, J. M. Gaines, and W. J. M. de Jonge (1998), A ferromagnetic resonance study on ultra-thin Fe_3O_4 layers grown on (001) MgO, *J. Magn. Magn. Mater.*, *182*, 71–80.

Verwey, E. J. W. (1939), Electronic conduction of magnetite (Fe_3O_4) and its transition point at low temperature, *Nature*, *144*, 327–328.

Walz, F. (2002), The Verwey transition—A topical review, *J. Phys. Condens. Matter*, *14*, R285–R340.

Walz, F., and H. Kronmüller (1991), Evidence for a single-stage Verwey-transition in perfect magnetite, *Philos. Mag. B*, *84*, 623–628.

Walz, F., V. A. M. Brabers, and H. Kronmueller (1997), Analysis of magnetite and related ferrites by means of magnetic aftereffect spectra, *J. Phys. IV*, *7*, 569–572.

Walz, F., V. A. M. Brabers, J. H. V. J. Brabers, and H. Kronmüller (2005), Timescale settling and nature of electron transport in magnetite—General considerations in view of new magnetic after-effect on dilutely Ti^{4+}-doped Fe_3O_4, *J. Phys. Condens. Matter*, *17*, 6763–6781.

Wieser, H. G., and M. G. Yasargil (1981), Selective amygdala-hippocampectomy as a surgical-treatment of mesiobasal limbic psychomotor epilepsy, *Electroencephalogr. Clin. Neurophysiol.*, *51*, P71.

F. Brem and A. M. Hirt, Institute of Geophysics, ETH-Zürich, Schafmattstrasse 30, CH-8903 Zürich, Switzerland. (hirt@mag.ig.erdw.ethz.ch)

D. Faivre, Max Planck Institute for Marine Microbiology, Celciusstrasse 1, D-28359 Bremen, Germany.

M. Hanzlik, Technische Chemie 1, TU München, Lichtenbergstrasse 4, D-85748 Gärching, Germany.